Ca²⁺-activated Cl⁻ current is antiarrhythmic by reducing both spatial and temporal heterogeneity of cardiac repolarization

Bence Hegyi[a,b,1], **Balázs Horváth**[a,c,1], **Krisztina Váczi**[a], **Mónika Gönczi**[a,d], **Kornél Kistamás**[a], **Ferenc Ruzsnavszky**[a], **Roland Veress**[a], **Leighton T. Izu**[c], **Ye Chen-Izu**[c,e,f], **Tamás Bányász**[a], **János Magyar**[a,g], **László Csernoch**[a], **Péter P. Nánási**[a,h,*], and **Norbert Szentandrássy**[a,h]

[a]Department of Physiology, Faculty of Medicine, University of Debrecen, Nagyerdei krt 98, P.O. Box 22, H-4012 Debrecen, Hungary

[b]Department of Pharmacology, Genome and Biomedical Science Facility, University of California, Davis, 451 Health Sciences Drive, Rm 3503, Davis, CA 95616, USA

[c]Faculty of Pharmacy, University of Debrecen, Nagyerdei krt 98, P.O. Box 22, H-4012 Debrecen, Hungary

[d]MTA-DE Momentum, Laboratory of Protein Dynamics, Department of Biochemistry and Molecular Biology, Faculty of Medicine, University of Debrecen, Nagyerdei krt 98, P.O. Box 22, H-4012 Debrecen, Hungary

[e]Department of Biomedical Engineering, Genome and Biomedical Science Facility, University of California, Davis, 451 Health Sciences Drive, Rm 2303, Davis, CA 95616, USA

[f]Department of Internal Medicine, Division of Cardiology, Genome and Biomedical Science Facility, University of California, Davis, 451 Health Sciences Drive, Rm 6315, Davis, CA 95616, USA

[g]Division of Sport Physiology, Department of Physiology, Faculty of Medicine, University of Debrecen, Nagyerdei krt 98, P.O. Box 22, H-4012 Debrecen, Hungary

[h]Department of Dental Physiology and Pharmacology, Faculty of Dentistry, University of Debrecen, Nagyerdei krt 98, P.O. Box 22, H-4012 Debrecen, Hungary

Abstract

The role of Ca^{2+}-activated Cl^- current ($I_{Cl(Ca)}$) in cardiac arrhythmias is still controversial. It can generate delayed afterdepolarizations in Ca^{2+}-overloaded cells while in other studies incidence of early afterdepolarization (EAD) was reduced by $I_{Cl(Ca)}$. Therefore our goal was to examine the role of $I_{Cl(Ca)}$ in spatial and temporal heterogeneity of cardiac repolarization and EAD formation.

Experiments were performed on isolated canine cardiomyocytes originating from various regions of the left ventricle; *subepicardial*, *midmyocardial* and *subendocardial* cells, as well as *apical* and

*Corresponding author at: Department of Physiology, University of Debrecen, Nagyerdei krt 98, P.O. Box 22, H-4012 Debrecen, Hungary. nanasi.peter@med.unideb.hu (P.P. Nánási).

[1]These authors have equally contributed.

basal cells of the midmyocardium. $I_{Cl(Ca)}$ was blocked by 0.5 mmol/L 9-anthracene carboxylic acid (9-AC). Action potential (AP) changes were tested with sharp microelectrode recording. Whole-cell 9-AC-sensitive current was measured with either square pulse voltage-clamp or AP voltage-clamp (APVC). Protein expression of TMEM16A and Bestrophin-3, ion channel proteins mediating $I_{Cl(Ca)}$, was detected by Western blot.

9-AC reduced phase-1 repolarization in every tested cell. 9-AC also increased AP duration in a reverse rate-dependent manner in all cell types except for subepicardial cells. Neither $I_{Cl(Ca)}$ density recorded with square pulses nor the normalized expressions of TMEM16A and Bestrophin-3 proteins differed significantly among the examined groups of cells. The early outward component of $I_{Cl(Ca)}$ was significantly larger in subepicardial than in subendocardial cells in APVC setting. Applying a typical subepicardial AP as a command pulse resulted in a significantly larger early outward component in both subepicardial and subendocardial cells, compared to experiments when a typical subendocardial AP was applied.

Inhibiting $I_{Cl(Ca)}$ by 9-AC generated EADs at low stimulation rates and their incidence increased upon beta-adrenergic stimulation. 9-AC increased the short-term variability of repolarization also.

We suggest a protective role for $I_{Cl(Ca)}$ against risk of arrhythmias by reducing spatial and temporal heterogeneity of cardiac repolarization and EAD formation.

Keywords

Ca^{2+}-activated Cl^- current; TMEM16A; Bestrophin-3; Spatial heterogeneity of repolarization; Short-term variability of repolarization; Early afterdepolarization

1. Introduction

In cardiac arrhythmias the regular electrical activity of the heart is altered. Some of these arrhythmias can be life-threatening tachyarrhythmias like torsades de pointes ventricular tachycardia (TdP) and ventricular fibrillation (VF). These tachyarrhythmias can result in sudden cardiac death which is the major cause of mortality in Europe and in the USA [1,2].

Cardiac action potentials (APs) characteristically differ between regions of the working myocardium. Inhomogeneity of repolarization is a peculiarity of even healthy myocardium and includes transmural dispersion of repolarization [3], the apico-basal gradient in repolarization [4] as well as different repolarization times in left versus right ventricular muscle [5]. This regional heterogeneity contributes to development of ECG waves [6] whereas the increase of this heterogeneity is considered to be arrhythmogenic by possible reentry formation [7,8].

QT interval prolongation is considered as a risk factor of cardiac arrhythmias as it promotes the development of the highly arrhythmogenic early afterdepolarizations (EADs) and TdP [9]. Short-term variability of repolarization has a higher predictive value than the extent of QT interval prolongation [10]. This temporal heterogeneity of repolarization can be measured on isolated cells and monitored as the variability of ventricular AP duration (APD) [11,12].

Abnormalities of intracellular Ca^{2+} homeostasis (Ca^{2+} overload and spontaneous Ca^{2+} release from the sarcoplasmic reticulum (SR)) may also influence the onset of TdP [13]. Spontaneous SR Ca^{2+} release activates the Ca^{2+} removal mechanisms of the cell generating a transient inward current leading to membrane depolarization (delayed afterdepolarization, DAD) and triggered activity. The source of the transient inward current can be the Na^+/Ca^{2+} exchange current (I_{NCX}) operating in forward mode or the activation of Ca^{2+}-activated Cl^- current ($I_{Cl(Ca)}$) [14,15].

$I_{Cl(Ca)}$ is present in mammalian myocardium where it contributes to early repolarization [16] and to DAD formation at least in Ca^{2+}-overloaded cells [15,17]. On the contrary, incidence of both EADs and DADs evoked by various stimulations was increased in the presence of 9-anthracene carboxylic acid (9-AC), an inhibitor of $I_{Cl(Ca)}$ in canine ventricular cells [18] suggesting an antiarrhythmic role for $I_{Cl(Ca)}$. Similarly, $I_{Cl(Ca)}$ may play an important role in the prevention of arrhythmias in acidosis in rabbit ventricular myocytes [19]. This however was not the case in an ovine EAD model where 4,4′-diisothiocyanostilbene-2,2′-disulfonic acid (DIDS), another inhibitor of $I_{Cl(Ca)}$, barely had any action [20]. These conflicting results need further clarification to determine the pro-, or antiarrhythmic role of $I_{Cl(Ca)}$.

The molecular identity of $I_{Cl(Ca)}$ is still controversial but TMEM16A (also known as Anoctamin1 or Ano1) [21–23] and Bestrophins are the most likely candidates, the latter ones at least as the Ca^{2+}-sensitive channel subunits [24]. More and more information is available on the physiological functions of TMEM16 in smooth muscle [25], neuronal and other tissues [26]. Moreover, TMEM16A is expressed in murine ventricle and it was confirmed to be responsible for $I_{Cl(Ca)}$ in ventricular myocytes [27]. Previously we have confirmed the expression of TMEM16A and Bestrophin-3 on both canine and human isolated left ventricular cardiomyocytes [28]. It was also shown that these two proteins co-localize with each other and $Ca_v1.2$ suggesting a direct control of $I_{Cl(Ca)}$ by Ca^{2+} entry through L-type Ca^{2+} channels (LTCCs) in canine ventricular myocytes [28]. Although a previous publication found no evidence for the existence of $I_{Cl(Ca)}$ in healthy human ventricular myocytes [29] but this was not confirmed later. Only two other publications used human cells but in both studies the examined cells were obtained from patients with end-stage heart failure [20,30] and only extrapolated to healthy human tissue from the fact that heart failure does not change the density of $I_{Cl(Ca)}$ in sheep ventricle [20].

The goal of our study was to assess the possible role of $I_{Cl(Ca)}$ in spatial and temporal heterogeneity of cardiac repolarization using two techniques which are probably the closest to physiological conditions.

First, conventional sharp microelectrode recordings were performed to assess the role of $I_{Cl(Ca)}$ on AP of cells isolated from various regions of the left ventricular myocardium (subepicardial, midmyocardial and subendocardial layers and the apical and basal parts of the midmyocardial layer). Second, action potential voltage-clamp (APVC) technique was used to record $I_{Cl(Ca)}$ profiles as 9-AC-sensitive current (I_{9-AC}) under experimental conditions designed to closely mimic physiological conditions (with preserved intracellular Ca^{2+} homeostasis). The normalized expression of TMEM16A and Bestrophin-3 proteins

were calculated from Western blot images performed on isolated myocytes obtained from the previously mentioned regions.

Our results indicate that $I_{Cl(Ca)}$ reduces both regional (transmural and apico-basal) and temporal (short-term variability of APD) heterogeneity of repolarization suggesting an antiarrhythmic role for the current. Neither $I_{Cl(Ca)}$ density recorded with square pulses nor the normalized expressions of TMEM16A and Bestrophin-3 proteins differed significantly among the examined cells of various origin. $I_{Cl(Ca)}$ densities measured with APVC in subepicardial cells were larger than that in subendocardial ones probably due to the larger Ca^{2+} entry through LTCCs during subepicardial APs.

2. Methods

A detailed description of the applied methods including electrophysiology protocols, composition of solutions, molecular biological reagents, etc. is provided in the Online Supplement.

All animal handling and laboratory procedures conform to the Guide for the Care and Use of Laboratory Animals published by the US National Institutes of Health (NIH publication no. 85-23, revised 1996), and to our Institutional Animal Care and Use Committee approved protocols (license no. 10/2011/DEMÁB). Chemicals and reagents were purchased from Sigma-Aldrich Co. (St. Louis, MO, USA) if not specified otherwise. All experiments except for molecular biological techniques were performed at 37 °C and pH = 7.4.

Experiments were performed in enzymatically isolated myocytes obtained from various regions of the canine left ventricle. Following digestion, thin slices were peeled off from both epicardial and endocardial surfaces of the left ventricle containing subepicardial (EPI) and subendocardial (ENDO) cells, respectively. Midmyocardial (MID) cells were obtained from the middle portion of the left ventricular free wall. In separate experiments, cells were collected from the apical and basal parts of the midmyocardial layer of the left ventricular wall.

APs were measured with sharp microelectrode recording during steady-state stimulation. Ionic currents were recorded using conventional whole-cell voltage clamp and APVC techniques. In the latter case the cell's own action potential was used as a command signal to record current profiles. $I_{Cl(Ca)}$ was dissected using 0.5 mmol/L 9-AC and presented as I_{9-AC} (Supplementary Fig. 1). 9-AC is suitable to study $I_{Cl(Ca)}$ as it evoked maximal effect on AP in 0.5 mmol/L concentration and did not alter L-type Ca^{2+} current ($I_{Ca,L}$), I_{Kr}, the slow component of delayed rectifier K^+ current (I_{Ks}), and the inward rectifier K^+ current (I_{K1}) [31]. Moreover, neither the transient outward K^+ current (I_{to1}) nor the intracellular Ca^{2+} concentration ($[Ca^{2+}]_i$) was influenced by 0.5 mmol/L 9-AC (Supplementary Fig. 2). Furthermore, 9-AC-sensitive current recorded in rabbit myocytes was completely different from apamin-sensitive current (Supplementary Fig. 3) but identical to the CaCCinh-A01-sensitive current (Supplementary Fig. 4) suggesting the lack of 9-AC action on small conductance Ca^{2+}-activated K^+ current (I_{SK}) channels and the suitability of 9-AC for the study of $I_{Cl(Ca)}$.

Short-term variability of repolarization (SV) was evaluated from a series of 50 consecutive APs evoked by 1 Hz steady-state stimulation and presented in Poincaré diagrams to visualize drug-induced changes in SV as previously [12]. The overall probability of differences between consecutive APD_{90} values in each cell was averaged and plotted (Fig. 6E, F) to illustrate any changes in SV.

Protein expression of TMEM16A and Bestrophin-3 was detected by Western blot in samples obtained from the previously mentioned five types of isolated ventricular myocytes.

All values are presented as arithmetic means ± Standard Error of the Mean (SEM). The number of cells in each experimental group was reported in the figures, and the cells in each group came from at least three animals. Given the biological variability among cells, each cell was treated as independent in the statistical tests, although more cells could be obtained from the same animal. Statistical significance of differences was evaluated using one-way ANOVA to compare multiple groups and Bonferroni posttest was used for pairwise comparisons. Statistical significance of a treatment was evaluated using Student's paired *t*-test. Differences were considered significant when p was less than 0.05 and indicated with either asterisks or + symbols.

3. Results

3.1. The contribution of $I_{Cl(Ca)}$ to the AP contour differs in various transmural layers of canine left ventricular myocardium

First the effect of $I_{Cl(Ca)}$ inhibition achieved by 0.5 mmol/L 9-AC was evaluated in isolated myocytes obtained from various layers of the left ventricular anterior wall (Fig. 1). After the stabilization of the AP shape, APs were recorded in steady-state conditions starting with 5 s cycle length (CL), and then procedure was repeated using progressively smaller CLs in control solution. After recording steady-state APs at five different CLs the CL was changed back to 5 s and 9-AC was perfused. When the effect of 9-AC developed (typically 7–8 min) the AP recordings at changing CLs were repeated as before. Finally the washout of the inhibitor was performed to test the reversibility of 9-AC-induced AP changes.

9-AC reduced phase-1 repolarization of AP in all cell types studied (Fig. 1A-C, 1E). $I_{Cl(Ca)}$ inhibition increased APD_{90} in MID and ENDO cells (Fig. 1A-B, F) but did not significantly change APD_{90} values of EPI cells (Fig. 1C, F). Action potential duration was altered by 9-AC in a reverse rate-dependent manner in MID and ENDO cells (Fig. 1F). Every 9-AC-induced change of AP parameters was reversible within the 10–15 min of washout (Fig. 1A-C). Resting membrane potential (RMP) and V_{max} values were not altered by 9-AC.

To study the possible reasons of the observed transmural differences of 9-AC-induced AP changes, 1 mmol/L 4-aminopyridine (4-AP, inhibitor of I_{to1}) was applied in EPI cells to reduce phase-1. This intervention altered the AP contour of EPI cells in a way that it became similar to APs of ENDO cells (Fig. 1D). The application of 9-AC in the continuous presence of 4-AP altered AP parameters the same way as it was observed in ENDO cells (Fig. 1E-G) namely 9-AC prolonged APD in 4-AP pretreated EPI cells. AP parameters (mean ± SEM values) measured in the absence and presence of 9-AC are summarized in Table 1.

3.2. Apico-basal differences in 9-AC-induced changes of AP parameters

Similar experiments were performed on cells isolated from the apical and basal parts of the left ventricular midmyocardium. APD_{90} was increased while phase-1 repolarization was reduced by 9-AC similarly in both types of cells (Fig. 2). The reverse rate-dependent lengthening of AP was greater in basal cells and this difference was significant at 0.5 and 1 s CLs (Fig. 2D). In concordance with our results with cells isolated from various transmural layers, 9-AC had no influence on RMP and V_{max} values and its effects on AP parameters were reversible (Fig. 2A, B). AP parameters (mean ± SEM values) measured in apical and basal cells are summarized in Table 2.

3.3. Equal $I_{Cl(Ca)}$ densities, TMEM16A and Bestrophin-3 expression levels in cardiomyocytes obtained from various left ventricular regions

To examine the possible reason for the previously described differences in 9-AC-induced AP changes we looked for any potential differences in $I_{Cl(Ca)}$ densities and protein expression levels of TMEM16A and Bestrophin-3, the most likely candidates responsible for $I_{Cl(Ca)}$. 9-AC-sensitive current densities were measured using conventional square pulses in cells of various origin of the left ventricle (Fig. 3A). $I_{Cl(Ca)}$ densities were equal regardless of the origin of the studied cell. This was the case not only for the transmural (Fig. 3B) but also for the apico-basal (Fig. 3C) gradient. $I_{Cl(Ca)}$ started to activate at −20 mV and had its highest value at +60 mV in all studied cell types (Fig. 3B, C) similarly to our earlier studies [28,31].

The expression levels of both TMEM16A and Bestrophin-3 were detected together with that of β-actin (Fig. 3D). Similarly to current densities, equal expression levels were observed for both TMEM16A and Bestrophin-3 when normalized to β-actin expression in all studied cell types (Fig. 3E).

Based on the square pulse voltage clamp data and protein expression results, the previously seen differential 9-AC-induced AP changes could not due to the differences in channel expression.

3.4. Transmural heterogeneity of $I_{Cl(Ca)}$ profiles measured with APVC

To explain the cause of differences in 9-AC-induced AP changes among left ventricular cells of various origins we studied $I_{Cl(Ca)}$ profiles, recorded as I_{9-AC}, with APVC. Using this technique we could activate $I_{Cl(Ca)}$ with the previously recorded own AP of each studied cell as voltage command to test the importance of AP contour in the activation of the current. Moreover, the pipette solution did not contain any calcium buffers or Ca^{2+} so $[Ca^{2+}]_i$ was not altered artificially. I_{9-AC} profiles were similar in dynamics in each cell type derived from various transmural regions of the left ventricular wall regardless of the marked and well-known difference in the shape of the APs (Fig. 4A). I_{9-AC} profiles consisted from an early, large, and fast outward component corresponding to phase-1 of APs followed by a late, small, and inward component (Fig. 4B). However, both the peak current density and the normalized total charge values of the outward component were statistically larger in EPI cells compared to ENDO ones (Fig. 4C, D).

3.5. Dependence of $I_{Cl(Ca)}$ profiles on the shape of the AP

To further investigate the possible reason for the greater current peak and total charge values measured in EPI cells with APVC and the markedly different actions of 9-AC on APs of EPI cells the following strategy was used. Typical ENDO and EPI APs (Fig. 5A and B, respectively) were selected and used as voltage commands in APVC experiments in both ENDO and EPI cells. The theory behind this experiment was to test the importance of the shape of the AP command waveform in activation of $I_{Cl(Ca)}$. I_{9-AC} profiles were very similar in dynamics with both stimulus waveforms in both ENDO cells (Fig. 5C) and EPI cells (Fig. 5D). There was however a difference in the peak current density and total charge values of the early outward component as activating $I_{Cl(Ca)}$ with EPI waveforms always resulted in larger values independent from which cell type was used to record $I_{Cl(Ca)}$ (Fig. 5E, F).

3.6. Role of $I_{Cl(Ca)}$ in EAD generation and short-term variability of repolarization (SV)

EAD is a depolarization occurring before complete repolarization, during the plateau phase of the AP and considered to be responsible for the initiation of malignant cardiac arrhythmias [32]. During our experiments 0.5 mmol/L 9-AC induced EADs in a small percentage of cells only at long CL stimulation (Fig. 6A, B). Increasing $[Ca^{2+}]_i$ by the application of the non-specific β-adrenergic agonist isoproterenol (ISO, 10 nmol/L) did not evoke EADs at any studied CLs in the absence of 9-AC but the simultaneous application of the two compounds resulted in much higher EAD occurrence, especially at long CLs (Fig. 6B).

The *short-term variability* of QT interval has a better predictive value regarding the development of cardiac arrhythmias than the *duration* of the QT interval itself [9,10]. As QT interval corresponds to the duration of ventricular AP, short-term variability of QT interval can be represented as short-term variability of AP duration (SV) on the cellular level. It must be emphasized that these experiments were done at 1 Hz steady-state pacing, therefore the recorded changes in either APD or SV could not be due to EAD occurrence. To better illustrate SV, Poincaré diagrams are usually plotted where either the duration of APs (APD_{90}) or QT intervals are presented as a function of the previous APD_{90} or QT interval duration values. 9-AC increased APD_{90} whereas the addition of ISO abolished this AP prolongation (Fig. 6C). Average of SV values in the 24 studied cells was larger in the presence of 9-AC (3.1 ± 0.2 ms) but the addition of ISO reduced the SV to a smaller value (1.8 ± 0.2 ms) than that calculated in control condition (2.3 ± 0.1 ms) (inset of Fig. 6C). However, without 9-AC pretreatment ISO decreased SV to an even smaller value (1.4 ± 0.1 ms) (inset of Fig. 6D). Even more importantly, upon evaluating the dispersion of differences in consecutive APD_{90} values in the presence of 9-AC the cumulative distribution curve was shifted toward greater beat-to-beat variability, indicating the increase of differences in consecutive APD_{90} values (Fig. 6E, F).

4. Discussion

4.1. Influence of $I_{Cl(Ca)}$ on AP configuration and spatial heterogeneity of repolarization

Similarly to our previous study [31] 9-AC did not modify V_{max} in any studied cell type (Tables 1 and 2) indicating its lack of action on fast Na^+ current. This makes the drug

suitable for studying the role of $I_{Cl(Ca)}$ even during AP measurements. 9-AC prolonged APD in both ENDO and MID cells (Fig. 1A, B and F) in line with previous findings [18,31]. In EPI cells, however, there was no AP prolongation (Fig. 1C, F). This can be due to a possible shortening effect induced by I_{Kr} accumulation and also by a smaller Ca^{2+} influx in the absence of a pronounced spike and dome AP configuration [33]. This AP shortening seems to overcome the AP prolongation likely induced by 9-AC. Phase-1 repolarization was reduced by 9-AC in all studied cell types (Fig. 1A-E). Upon the reduction of phase-1 (by partial blockade of I_{to1} achieved by 1 mmol/L 4-AP) the shape of the AP in EPI cells became similar to those of ENDO ones. When 9-AC was applied in this condition, changes of AP parameters became practically identical to those observed in ENDO cells (Fig. 1B, D-F). These results suggest that the lack of 9-AC action on APD of EPI cells were due to the pronounced spike and dome configuration of AP created by the large I_{to1} density in these cells [34]. This is in good agreement with the conclusion of Zygmunt et al. who suggested an important role for I_{to1} in the activation of subsequent ion currents like $I_{Cl(Ca)}$ and $I_{Ca,L}$ [35].

Our results are in good agreement with an earlier study [36] despite the differences in the experimental conditions. Verkerk et al. used DIDS to inhibit $I_{Cl(Ca)}$ in rabbit left ventricular myocytes measured with patch-clamp configuration while here 9-AC was applied during sharp microelectrode recording in canine left ventricular myocytes. Still, they found no AP prolongation in EPI cells except for the fastest stimulation rate of 3.33 Hz. Moreover, similarly to our observation, blockade of $I_{Cl(Ca)}$ prolonged the AP in EPI cells at 1 Hz only when DIDS was applied in the presence of I_{to1} inhibition [36]. A canine study reported similar findings to our results as APD was increased when phase-1 repolarization was slow and shallow (like in MID and ENDO cells) [35].

Blockade of $I_{Cl(Ca)}$ prolonged APD of MID, ENDO and also 4-AP pretreated EPI cells in a reverse rate-dependent manner (Fig. 1F). This concurs with our previous findings about rate-dependent changes of APD in canine [37] and in other mammalian species [38]. Moreover, two other factors might contribute to the 9-AC-induced, rate-dependent AP prolongation. One is the rate-dependent variation of $[Ca^{2+}]_i$ as it was shown that $[Ca^{2+}]_i$ is larger upon the increase of stimulation rate both during steady-state [31] as well as without steady-state [34]. Moreover, $[Ca^{2+}]_i$ correlates well with $I_{Cl(Ca)}$ measured as I_{9-AC} with square pulses [31]. Another factor is the rate-dependent behavior of I_{to1} density as the availability of its channels reduces at fast stimulation rates due to the relatively slow recovery from inactivation [34]. This is reflected in the fact that phase-1 showed rate-dependent properties in control conditions as it was larger at long CLs. Moreover, this rate-dependence was also present when $I_{Cl(Ca)}$ was blocked by 9-AC in all five studied cell types (not shown). Therefore, the rate-dependence of phase-1 seems to be rather modulated by the recovery from inactivation kinetics of I_{to1} than the magnitude of $I_{Cl(Ca)}$. This emphasizes that reverse rate dependency is an intrinsic property of the myocardium [38]. Therefore, similarly to the study performed on rabbit cells [36] the role of $I_{Cl(Ca)}$ in the reduction of transmural APD heterogeneity is more pronounced at slow heart rates. This makes the contribution of $I_{Cl(Ca)}$ even more important as the heterogeneity of repolarization is the greatest at slow stimulation rates [39].

Our study is the first to describe the apico-basal contribution of $I_{Cl(Ca)}$ to AP configuration (Fig. 2). Our baseline AP parameters were similar to those published earlier [4] and 9-AC-induced changes of AP parameters in the apico-basal direction were similar to those observed in the transmural direction. Again, the heterogeneity of AP repolarization was reduced by $I_{Cl(Ca)}$ and this action was the strongest at slow stimulation rates (Fig. 2D).

4.2. Transmural difference in $I_{Cl(Ca)}$ and its underlying ion channel proteins

$I_{9\text{-}AC}$ could be used to explore the contribution of $I_{Cl(Ca)}$ to the AP in closely physiological conditions (without the application of intracellular Ca^{2+} buffering during APVC) [28]. Regional differences, however, were not studied previously with APVC despite some earlier studies where either a "typical" AP was applied as the command signal during perforated patch recording using nonspecific blockers to dissect $I_{Cl(Ca)}$ [35] or 10 mmol/L EGTA was applied in the pipette solution interfering with physiological Ca^{2+} homeostasis [18]. The current density of $I_{9\text{-}AC}$ early outward component was statistically larger in EPI cells compared to what was recorded in ENDO ones (Fig. 4C, D). This EPI-ENDO difference was unexpected as a previous study did not report any transmural difference in $I_{Cl(Ca)}$ density in the canine left ventricle [40]. It must be noted that the result of that study is in full agreement with our results as $I_{Cl(Ca)}$ densities of EPI and MID cells were compared. $I_{Cl(Ca)}$ was not studied in ENDO cells and conventional square pulses were used with the application of the nonspecific blocker (4-acetamido-4′-isothiocyanostilbene-2,2′-disulfonic acid) of the current [40]. Similarly, although 9-AC was used both during APVC and conventional voltage-clamp measurements, in the latter case no difference was found in $I_{Cl(Ca)}$ densities of cells obtained from various transmural layers just as upon comparing midmyocardial cells from apical or basal origin (Fig. 3B, C). In line with this, the densities of TMEM16A and Bestrophin-3 proteins (two likely candidates for mediating $I_{Cl(Ca)}$ [21–24]) both normalized to β-actin were equal regardless of the origin of the samples (Fig. 3E). In contrast to present results, the amplitude of $I_{Cl(Ca)}$ measured with square wave voltage clamp was significantly greater in feline epicardial cells compared to endocardial ones [41] suggesting a potential interspecies difference.

4.3. Larger $I_{Cl(Ca)}$ density of EPI cells is determined by the contour of AP

The current density of $I_{9\text{-}AC}$ early outward component was statistically larger in EPI cells than that of ENDO ones in APVC conditions (Fig. 4C) and 9-AC induced AP prolongation in ENDO but not in EPI cells (Fig. 1F). On the contrary, $I_{9\text{-}AC}$ density was equal with square pulse voltage-clamp measurements (Fig. 4A). It must be noted that during square pulse measurements the stimulus waveform is quite different from the physiological one. Under APVC, however, the previously recorded, own AP was used for physiological stimulation on each studied cell. To test the hypothesis that the AP waveform could be responsible for the larger $I_{Cl(Ca)}$ density of EPI cells we used two previously recorded characteristic ENDO (Fig. 5A) and EPI (Fig. 5B) AP waveforms. ENDO AP possessed only a slow and small phase-1 (Fig. 5A) whereas EPI AP had a rapid and large phase-1 followed by a pronounced dome (Fig. 5B). Observations were consistent with our hypothesis as the characteristic EPI AP waveform induced a larger early outward $I_{Cl(Ca)}$ current than the ENDO AP waveform no matter whether the waveforms were applied on EPI or ENDO cells (Fig. 5C-F). These results can be explained based on what our group has previously found in case of the

nisoldipine-sensitive current on canine and human left ventricular myocytes [33,42]. It was shown that the charge carried by the nisoldipine-sensitive current was significantly larger during EPI AP compared to ENDO one [33]. This could result in a greater activation of $I_{Cl(Ca)}$ during the early phase of the AP. It is hard to predict the exact mechanism as the membrane potential also influences the activation of $I_{Cl(Ca)}$ beside the $[Ca^{2+}]_{cleft}$. Although the existence of a marked phase-1 during the EPI AP favors the entry of Ca^{2+} due to its increased driving force and the I–V characteristics of the LTCCs but this more negative membrane potential actually acts against Cl^- influx. Nevertheless, it seems that the overall action of a more pronounced phase-1 (EPI AP) is the increase of the early outward component of $I_{Cl(Ca)}$. This larger current is definitely not due to the increased density of channel proteins in EPI cells as the expression of TMEM16A and Bestrophin-3 was equal in both transmural and apico-basal direction (Fig. 4D). Although the expression level of $Ca_v1.2$, the pore-forming subunit of LTCCs was not studied in ENDO cells but it was equal in EPI and MID cells [43], similarly to the equal density of TMEM16A and Bestrophin-3 described in the present study.

4.4. Influence of $I_{Cl(Ca)}$ on temporal variability of cardiac repolarization and EAD formation

Prolongation of repolarization is considered as a risk factor of cardiac arrhythmias as it can lead to EADs and TdP [9]. The short-term variability of repolarization is considered to be even more important as a predictor of cardiac arrhythmias highlighted by a position statement and consensus guidance were endorsed by the European Heart Rhythm Association jointly with the ESC Working Group on Cardiac Cellular Electrophysiology recently [44].

According to the previously mentioned studies, any SV reducing intervention could have an antiarrhythmic property. It must be emphasized that all of our experiments where SV was calculated were done at 1 Hz steady-state pacing, therefore the recorded changes in either APD or SV could not be due to EAD occurrence. The application of 9-AC induced an increase in SV (inset of Fig. 6C) suggesting an antiarrhythmic role for $I_{Cl(Ca)}$. This antiarrhythmic property of $I_{Cl(Ca)}$ is further supported by the fact that EADs were detected upon the blockade of $I_{Cl(Ca)}$ (in the presence of 9-AC, Fig. 6B). Another evidence supporting the antiarrhythmic role of $I_{Cl(Ca)}$ is the even larger EAD incidence in the simultaneous presence of 9-AC and ISO. ISO is well known to increase $[Ca^{2+}]_i$ and therefore most probably $[Ca^{2+}]_{cleft}$ as well. This leads to a larger $I_{Cl(Ca)}$ [28] which upon its blockade by 9-AC leads to a greater EAD incidence (Fig. 6B).

The value of SV calculated with the formula used in this study and also in earlier publications [12,45] is not necessarily the most sensitive way to indicate if the APD of only a few beats greatly differ from the average. This is especially the case when the APD of 50 consecutive APs are used. However, a large, sudden change in consecutive APD values occurring in a non-uniform manner in cells of various origins within the myocardium will more effectively trigger an arrhythmic event than a gradual and simultaneous increase in APD during the development of the action of a drug [8]. Therefore the difference between consecutive APD values were grouped in ms ranges and the overall probability of their appearance was calculated (Fig. 6E, F) in order to detect any unusually short or long AP

among the 50 analyzed one more easily. Using this analysis, 9-AC shifted the curve to the right, indicating an increase of differences between consecutive APD values, hence an arrhythmogenic effect. Moreover, the protective effect of ISO was smaller in the presence of 9-AC as the leftward shift of the curve by ISO was greater in the absence than in the presence of 9-AC. Similarly, in the presence of ISO the value of SV was smaller when 9-AC was not applied (Fig. 6G). Therefore it seems that $I_{Cl(Ca)}$ contributes to the ISO induced reduction of SV. These results all support a protective role of $I_{Cl(Ca)}$ against cardiac arrhythmia together with the previously mentioned spatial reduction of APD heterogeneity.

Our previous study is congruent with the current results as a protective role of $I_{Cl(Ca)}$ was suggested in cesium and ouabain induced canine ventricular myocyte EAD model as well [18]. In contrast, on sheep ventricular cells DIDS barely had any action on parameters of EADs [20]. Apart from the different species, the ovine study used norepinephrine to provoke EADs and studied the action of DIDS, a non-specific blocker of $I_{Cl(Ca)}$ which also inhibits Na^+ channels [31] on various parameters of EADs. In the current study, however, EADs were not provoked but their incidence was studied in the absence or presence of 9-AC, a more specific blocker of $I_{Cl(Ca)}$. Due to these differences it is rather hard to compare these studies.

It must be mentioned that DAD formation can also provoke cardiac arrhythmias by initiating TdP [13]. DADs can be produced not only by the forward mode I_{NCX} but also by $I_{Cl(Ca)}$ at least in some species and cell types. Indeed, it was shown that activation of $I_{Cl(Ca)}$ can be responsible for DAD generation in Ca^{2+}-overloaded canine ventricular [15], rabbit atrial, ventricular and Purkinje [14] and ovine Purkinje and ventricular [46] cells. The presence of ISO-induced chloride current (and DADs) was not detected in canine ventricular cells [47] but in the same experimental conditions a membrane depolarization was described in isolated guinea pig ventricular myocytes [47]. It might be that the application of 1 μmol/L ISO for 20 s was not enough to induce Ca^{2+} overload in canine cells, hence activation of $I_{Cl(Ca)}$ and DADs in that study [47]. Similarly, we did not detect any DADs during our experiments even in the presence of ISO, indicating that 10 nmol/L ISO does not induce Ca^{2+} overload in canine ventricular myocytes. It was possible to generate DADs by overloading canine cells with Ca^{2+} using ISO, but it had to be applied in 100 times higher dose together with ouabain [17].

4.5. Summary and potential relevance

The major findings of the present study suggest a protective role for $I_{Cl(Ca)}$ against risk of arrhythmias in the canine left ventricular myocardium. $I_{Cl(Ca)}$ achieves this by the reduction of both spatial and temporal heterogeneity of repolarization. As it was suggested earlier inhibition of $I_{Cl(Ca)}$ could be useful to reduce the Ca^{2+} overload induced DADs. At the same time, however, the blockade of $I_{Cl(Ca)}$ might increase the risk of cardiac arrhythmias by increasing spatial and temporal heterogeneity of repolarization and EAD formation. As it was shown the incidence of EAD formation was even higher when the blockade of $I_{Cl(Ca)}$ was established in the presence of ISO. Therefore, in a clinical setting where β-blockers are applied to reduce the heart rate and Ca^{2+} overload, antiarrhythmic action of $I_{Cl(Ca)}$ could be

even more pronounced as $I_{Cl(Ca)}$ reduces APD heterogeneity at slow heart rates more effectively.

Supplementary Material

Refer to Web version on PubMed Central for supplementary material.

Acknowledgments

Appendix A. Supplementary data

Supplementary data to this article can be found online at http://dx. doi.org/10.1016/j.yjmcc. 2017.06.014.

Abbreviations

4-AP	4-aminopyridine
9-AC	9-anthracene carboxylic acid
AP	action potential
APD	action potential duration
APD$_{90}$	action potential duration at 90% of repolarization
APVC	action potential voltage-clamp
Ca$_v$1.2	pore forming subunit of L-type Ca^{2+} channel
[Ca^{2+}]$_{cleft}$	Ca^{2+} concentration in the dyadic cleft
[Ca^{2+}]$_i$	intracellular Ca^{2+} concentration in bulk cytoplasm
CL	cycle length
DAD	delayed afterdepolarization
DIDS	4,4′-diisothiocyanostilbene-2,2′-disulfonic acid

|	
EAD	early afterdepolarization
ENDO	subendocardial cell
EPI	subepicardial cell
$I_{9\text{-AC}}$	9-anthracene carboxylic acid-sensitive current
I_{Ca}	L, L-type Ca^{2+} current
$I_{Cl(Ca)}$	Ca^{2+}-activated Cl^- current
I_{K1}	inward rectifier K^+ current
I_{Kr}	rapid component of delayed rectifier K^+ current
I_{Ks}	slow component of delayed rectifier K^+ current
I_{NCX}	Na^+/Ca^{2+} exchange current
I_{SK}	small conductance Ca^{2+}-activated K^+ current
I_{to1}	transient outward K^+ current
ISO	isoproterenol
LQT2	type 2 long QT syndrome
LTCC	L-type Ca^{2+} channel
MID	midmyocardial cell
RMP	resting membrane potential
SR	sarcoplasmic reticulum
SV	short-term variability of repolarization
TdP	torsades de pointes ventricular tachycardia
V_{max}	maximal rate of depolarization

References

1. Huikuri HV, Castellanos A, Myerburg RJ. Sudden death due to cardiac arrhythmias. N Engl J Med. 2001; 345:1473–1482. http://dx.doi.org/10.1056/NEJMra000650. [PubMed: 11794197]

2. Fishman GI, Chugh SS, Dimarco JP, Albert CM, Anderson ME, Bonow RO, et al. Sudden cardiac death prediction and prevention: report from a National Heart, Lung, and Blood Institute and Heart Rhythm Society Workshop. Circulation. 2010; 122:2335–2348. http://dx.doi.org/10.1161/CIRCULATIONAHA.110.976092. [PubMed: 21147730]

3. Liu DW, Gintant GA, Antzelevitch C. Ionic bases for electrophysiological distinctions among epicardial, midmyocardial, and endocardial myocytes from the free wall of the canine left ventricle. Circ Res. 1993; 72:671–687. http://dx.doi.org/10.1161/01.RES.72.3.671. [PubMed: 8431990]

4. Szentadrassy N, Banyasz T, Biro T, Szabo G, Toth BI, Magyar J, et al. Apico-basal inhomogeneity in distribution of ion channels in canine and human ventricular myocardium. Cardiovasc Res. 2005; 65:851–860. http://dx.doi.org/10.1016/j.cardiores.2004.11.022. [PubMed: 15721865]

5. Volders PG, Sipido KR, Carmeliet E, Spätjens RL, Wellens HJ, Vos MA. Repolarizing K^+ currents I_{TO1} and I_{Ks} are larger in right than left canine ventricular midmyocardium. Circulation. 1999; 99:206–210. http://dx.doi.org/10.1161/01.CIR.99.2.206. [PubMed: 9892584]

6. Antzelevitch C, Shimizu W, Yan GX, Sicouri S, Weissenburger J, Nesterenko VV, et al. The M cell: its contribution to the ECG and to normal and abnormal electrical function of the heart. J Cardiovasc Electrophysiol. 1999; 10:1124–1152. http://dx.doi.org/10.1111/j.1540-8167.1999.tb00287.x. [PubMed: 10466495]

7. Baláti B, Varró A, Papp JG. Pharmacological modification of the dispersion of repolarization in the heart: importance of the M cells. Cardiovasc Drugs Ther. 1999; 13:491–505. http://dx.doi.org/10.1023/A:1007819503060. [PubMed: 10686658]

8. Varró A, Baczkó I. Possible mechanisms of sudden cardiac death in top athletes: a basic cardiac electrophysiological point of view. Pflugers Arch. 2010; 460:31–40. http://dx.doi.org/10.1007/s00424-010-0798-0. [PubMed: 20186549]

9. Lengyel C, Varró A, Tábori K, Papp JG, Baczkó I. Combined pharmacological block of I_{Kr} and I_{Ks} increases short-term QT interval variability and provokes torsades de pointes. Br J Pharmacol. 2007; 151:941–951. http://dx.doi.org/10.1038/sj.bjp.0707297. [PubMed: 17533421]

10. Thomsen MB, Verduyn SC, Stengl M, Beekman JD, de Pater G, van Opstal J, et al. Increased short-term variability of repolarization predicts d-sotalol-induced torsades de pointes in dogs. Circulation. 2004; 110:2453–2459. http://dx.doi.org/10.1161/01.CIR.0000145162.64183.C8. [PubMed: 15477402]

11. Thomsen MB, Truin M, van Opstal JM, Beekman JD, Volders PG, Stengl M, et al. Sudden cardiac death in dogs with remodeled hearts is associated with larger beat-to-beat variability of repolarization. Basic Res Cardiol. 2005; 100:279–287. http://dx.doi.org/10.1007/s00395-005-0519-6. [PubMed: 15754087]

12. Szentandrássy N, Kistamás K, Hegyi B, Horváth B, Ruzsnavszky F, Váczi K, et al. Contribution of ion currents to beat-to-beat variability of action potential duration in canine ventricular myocytes. Pflugers Arch. 2015; 467:1431–1443. http://dx.doi.org/10.1007/s00424-014-1581-4. [PubMed: 25081243]

13. ter Bekke RM, Volders PG. Arrhythmogenic mechano-electric heterogeneity in the long-QT syndrome. Prog Biophys Mol Biol. 2012; 110:347–358. http://dx.doi.org/10.1016/j.pbiomolbio.2012.07.007. [PubMed: 22841828]

14. Szigeti G, Rusznak Z, Kovacs L, Papp Z. Calcium-activated transient membrane currents are carried mainly by chloride ions in isolated atrial, ventricular and Purkinje cells of rabbit heart. Exp Physiol. 1998; 83:137–153. http://dx.doi.org/10.1113/expphysiol.1998.sp004097. [PubMed: 9568474]

15. Zygmunt AC, Goodrow RJ, Weigel CM. I_{NaCa} and $I_{Cl(Ca)}$ contribute to isoproterenol-induced delayed after depolarizations in midmyocardial cells. Am J Phys. 1998; 275:H1979–H1992.

16. Zygmunt AC, Gibbons WR. Properties of the calcium-activated chloride current in heart. J Gen Physiol. 1992; 99:391–414. http://dx.doi.org/10.1085/jgp.99.3.391. [PubMed: 1375275]

17. Collier ML, Levesque PC, Kenyon JL, Hume JR. Unitary Cl^- channels activated by cytoplasmic Ca^{2+} in canine ventricular myocytes. Circ Res. 1996; 78:936–944. http://dx.doi.org/10.1161/01.RES.78.5.936. [PubMed: 8620614]

18. Fülöp L, Fiák E, Szentandrássy N, Magyar J, Nánási PP, Bányász T. The role of transmembrane chloride current in afterdepolarisations in canine ventricular cardiomyocytes. Gen Physiol Biophys. 2003; 22:341–353. [PubMed: 14986885]

19. Hirayama Y, Kuruma A, Hiraoka M, Kawano S. Calcium-activated CL^- current is enhanced by acidosis and contributes to the shortening of action potential duration in rabbit ventricular myocytes. Jpn J Physiol. 2002; 52:293–300. http://dx.doi.org/10.2170/jjphysiol.52.293. [PubMed: 12230806]

20. Verkerk AO, Tan HL, Kirkels JH, Ravesloot JH. Role of Ca^{2+}-activated Cl^- current during proarrhythmic early afterdepolarizations in sheep and human ventricular myocytes. Acta Physiol Scand. 2003; 179:143–148. http://dx.doi.org/10.1046/j.1365-201X.2003.01190.x. [PubMed: 14510777]

21. Caputo A, Caci E, Ferrera L, Pedemonte N, Barsanti C, Sondo E, et al. TMEM16A, a membrane protein associated with calcium-dependent chloride channel activity. Science. 2008; 322:590–594. http://dx.doi.org/10.1126/science.1163518. [PubMed: 18772398]

22. Yang YD, Cho H, Koo JY, Tak MH, Cho Y, Shim WS, et al. TMEM16A confers receptor-activated calcium-dependent chloride conductance. Nature. 2008; 455:1210–1215. http://dx.doi.org/10.1038/nature07313. [PubMed: 18724360]

23. Schroeder BC, Cheng T, Jan YN, Jan LY. Expression cloning of TMEM16A as a calcium-activated chloride channel subunit. Cell. 2008; 134:1019–1029. http://dx.doi.org/10.1016/j.cell.2008.09.003. [PubMed: 18805094]

24. Sun H, Tsunenari T, Yau KW, Nathans J. The vitelliform macular dystrophy protein defines a new family of chloride channels. Proc Natl Acad Sci U S A. 2002; 99:4008–4013. http://dx.doi.org/10.1073/pnas.052692999. [PubMed: 11904445]

25. Dam VS, Boedtkjer DM, Nyvad J, Aalkjaer C, Matchkov V. TMEM16A knockdown abrogates two different Ca^{2+}-activated Cl^- currents and contractility of smooth muscle in rat mesenteric small arteries. Pflugers Arch. 2014; 466:1391–1409. http://dx.doi.org/10.1007/s00424-013-1382-1. [PubMed: 24162234]

26. Pedemonte N, Galietta LJ. Structure and function of TMEM16 proteins (anoctamins). Physiol Rev. 2014; 94:419–459. http://dx.doi.org/10.1152/physrev.00039.2011. [PubMed: 24692353]

27. Ye Z, MM Wu, Wang CY, Li YC, CJ Yu, Gong YF, et al. Characterization of cardiac anoctamin1 Ca-activated chloride channels and functional role in ischemia-induced arrhythmias. J Cell Physiol. 2015; 230:337–346. http://dx.doi.org/10.1002/jcp.24709. [PubMed: 24962810]

28. Horváth B, Váczi K, Hegyi B, Gönczi M, Dienes B, Kistamás K, et al. Sarcolemmal Ca^{2+}-entry through L-type Ca^{2+} channels controls the profile of Ca^{2+}-activated Cl^- current in canine ventricular myocytes. J Mol Cell Cardiol. 2016; 97:125–139. http://dx.doi.org/10.1016/j.yjmcc.2016.05.006. [PubMed: 27189885]

29. Köster OF, Szigeti GP, Beuckelmann DJ. Characterization of a $[Ca^{2+}]_i$-dependent current in human atrial and ventricular cardiomyocytes in the absence of Na^+ and K^+ Cardiovasc Res. 1999; 41:175–187. http://dx.doi.org/10.1016/S0008-6363(98)00202-8. [PubMed: 10325965]

30. Verkerk AO, Veldkamp MW, Baartscheer A, Schumacher CA, Klöpping C, van Ginneken AC, et al. Ionic mechanism of delayed afterdepolarizations in ventricular cells isolated from human end-stage failing hearts. Circulation. 2001; 104:2728–2733. http://dx.doi.org/10.1161/hc4701.099577. [PubMed: 11723027]

31. Váczi K, Hegyi B, Ruzsnavszky F, Kistamás K, Horváth B, Bányász T, et al. 9-An-thracene carboxylic acid is more suitable than DIDS for characterization of calcium-activated chloride current during canine ventricular action potential. Naunyn Schmiedeberg's Arch Pharmacol. 2015; 388:87–100. http://dx.doi.org/10.1007/s00210-014-1050-9. [PubMed: 25344201]

32. Qu Z, Xie LH, Olcese R, Karagueuzian HS, Chen PS, Garfinkel A, et al. Early afterdepolarizations in cardiac myocytes: beyond reduced repolarization reserve. Cardiovasc Res. 2013; 99:6–15. http://dx.doi.org/10.1093/cvr/cvt104. [PubMed: 23619423]

33. Bányász T, Fülöp L, Magyar J, Szentandrássy N, Varró A, Nánási PP. Endocardial versus epicardial differences in L-type calcium current in canine ventricular myocytes studied by action potential voltage clamp. Cardiovasc Res. 2003; 58:66–75. http://dx.doi.org/10.1016/S0008-6363(02)00853-2. [PubMed: 12667947]

34. Litovsky SH, Antzelevitch C. Transient outward current prominent in canine ventricular epicardium but not endocardium. Circ Res. 1988; 62:116–126. http://dx.doi.org/10.1161/01.RES.62.1.116. [PubMed: 2826039]

35. Zygmunt AC, Robitelle DC, Eddlestone GT. I_{to1} dictates behavior of $I_{Cl(Ca)}$ during early repolarization of canine ventricle. Am J Phys. 1997; 273:H1096–H1106.

36. Verkerk AO, Tan HL, Ravesloot JH. Ca^{2+}-activated Cl^- current reduces transmural electrical heterogeneity within the rabbit left ventricle. Acta Physiol Scand. 2004; 180:239–247. http://dx.doi.org/10.1111/j.0001-6772.2003.01252.x. [PubMed: 14962005]

37. Bányász T, Horváth B, Virág L, Bárándi L, Szentandrássy N, Harmati G, et al. Reverse rate dependency is an intrinsic property of canine cardiac preparations. Cardiovasc Res. 2009; 84:237–244. http://dx.doi.org/10.1093/cvr/cvp213. [PubMed: 19556280]

38. Bányász T, Bárándi L, Harmati G, Virág L, Szentandrássy N, Márton I, et al. Mechanism of reverse rate-dependent action of cardioactive agents. Curr Med Chem. 2011; 18:3597–3606. http://dx.doi.org/10.2174/092986711796642355. [PubMed: 21774765]

39. Weissenburger J, Nesterenko VV, Antzelevitch C. Transmural heterogeneity of ventricular repolarization under baseline and long QT conditions in the canine heart in vivo: torsades de pointes develops with halothane but not pentobarbital anesthesia. J Cardiovasc Electrophysiol. 2000; 11:290–304. http://dx.doi.org/10.1111/j.1540-8167.2000.tb01798.x. [PubMed: 10749352]

40. Zygmunt AC. Intracellular calcium activates a chloride current in canine ventricular myocytes. Am J Phys. 1994; 267:H1984–H1995.

41. Furukawa T, Myerburg RJ, Furukawa N, Bassett AL, Kimura S. Differences in transient outward currents of feline endocardial and epicardial myocytes. Circ Res. 1990; 67:1287–1291. http://dx.doi.org/10.1161/01.RES.67.5.1287. [PubMed: 2225360]

42. Fülöp L, Bányász T, Magyar J, Szentandrássy N, Varró A, Nánási PP. Reopening of L-type calcium channels in human ventricular myocytes during applied epicardial action potentials. Acta Physiol Scand. 2004; 180:39–47. http://dx.doi.org/10.1046/j.0001-6772.2003.01223.x. [PubMed: 14706111]

43. Szabo G, Szentandrassy N, Biro T, Toth BI, Czifra G, Magyar J, et al. Asymmetrical distribution of ion channels in canine and human left-ventricular wall: epicardium versus midmyocardium. Pflugers Arch. 2005; 450:307–316. http://dx.doi.org/10.1007/s00424-005-1445-z. [PubMed: 15952036]

44. Baumert M, Porta A, Vos MA, Malik M, Couderc JP, Laguna P, et al. QT interval variability in body surface ECG: measurement, physiological basis, and clinical value: position statement and consensus guidance endorsed by the European Heart Rhythm Association jointly with the ESC Working Group on Cardiac Cellular Electrophysiology. Europace. 2016; 18:925–944. http://dx.doi.org/10.1093/europace/euv405. [PubMed: 26823389]

45. Johnson DM, Heijman J, Pollard CE, Valentin JP, Crijns HJ, Abi-Gerges N, et al. I_{Ks} restricts excessive beat-to-beat variability of repolarization during beta-adrenergic receptor stimulation. J Mol Cell Cardiol. 2010; 48:122–130. http://dx.doi.org/10.1016/j.yjmcc.2009.08.033. [PubMed: 19744496]

46. Verkerk AO, Veldkamp MW, Bouman LN, van Ginneken AC. Calcium-activated Cl⁻ current contributes to delayed afterdepolarizations in single Purkinje and ventricular myocytes. Circulation. 2000; 101:2639–2644. http://dx.doi.org/10.1161/01.CIR.101.22.2639. [PubMed: 10840017]

47. Sorota S, Siegal MS, Hoffman BF. The isoproterenol-induced chloride current and cardiac resting potential. J Mol Cell Cardiol. 1991; 23:1191–1198. http://dx.doi.org/10.1016/0022-2828(91)90207-3. [PubMed: 1749007]
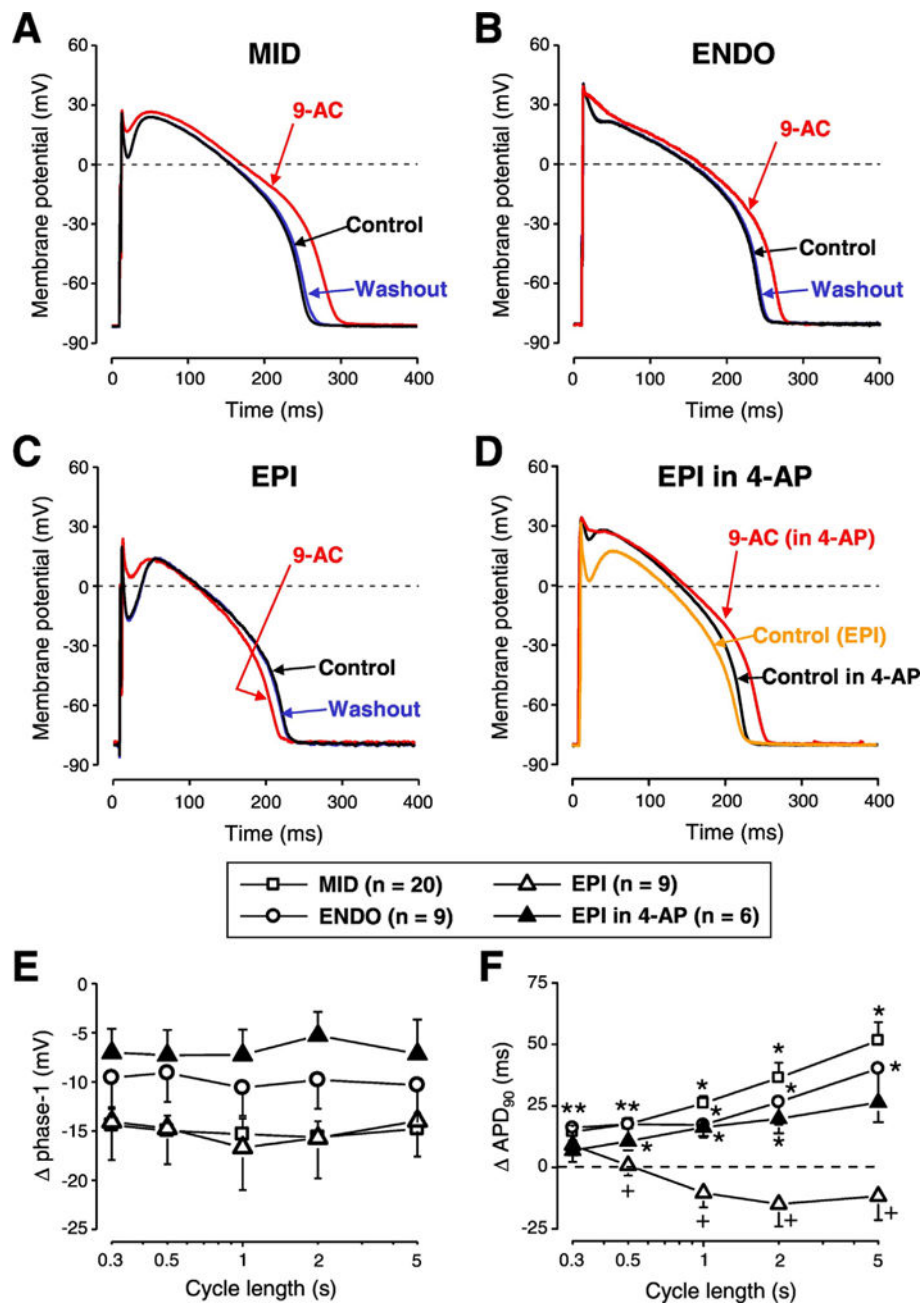
Fig. 1.
The contribution of $I_{Cl(Ca)}$ to the AP contour differs in various transmural layers of canine left ventricular myocardium. Representative APs recorded in control conditions (black), in the presence of 0.5 mmol/L 9-anthracene carboxylic acid (9-AC) (red) and after washout (blue) in cells obtained from midmyocardium (A, MID), subendocardium (B, ENDO) and subepicardium (C, EPI). Panel D shows a representative experiment where 9-AC was used in the presence of 1 mmol/L 4-aminopyridine (4-AP) in an EPI cell. 9-AC-induced changes in phase-1 (E) and APD_{90} (F) are shown in various cell types and conditions as indicated by the symbols. Symbols and bars represent mean ± SEM values, n shows the number of experiments. On panel E every 9-AC induced change in phase-1 was statistically significant.

On panels F asterisks denote 9-AC-induced significant changes while + signs indicate significant difference between EPI and EPI in the presence of 4-AP. (For interpretation of the references to colour in this figure legend, the reader is referred to the web version of this article.)
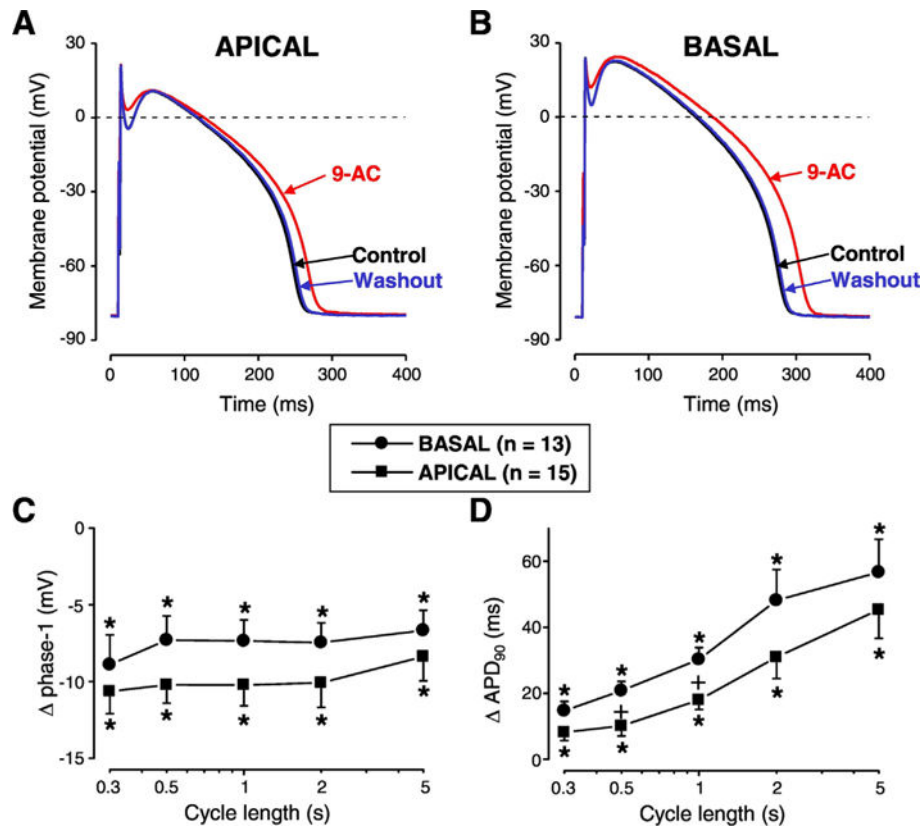
Fig. 2.
Apico-basal differences of 9-AC-induced AP changes. Reversible AP changes induced by 9-AC in cells obtained from apical (A) and basal cells (B) of canine left ventricular midmyocardium. Frequency-dependent changes in phase-1 (C) and APD$_{90}$ (D) were measured in apical (squares) and basal cells (circles). Symbols and bars represent mean ± SEM values. Asterisks denote significant 9-AC-induced changes. + signs indicate significant difference between apical and basal cells, n shows the number of experiments.
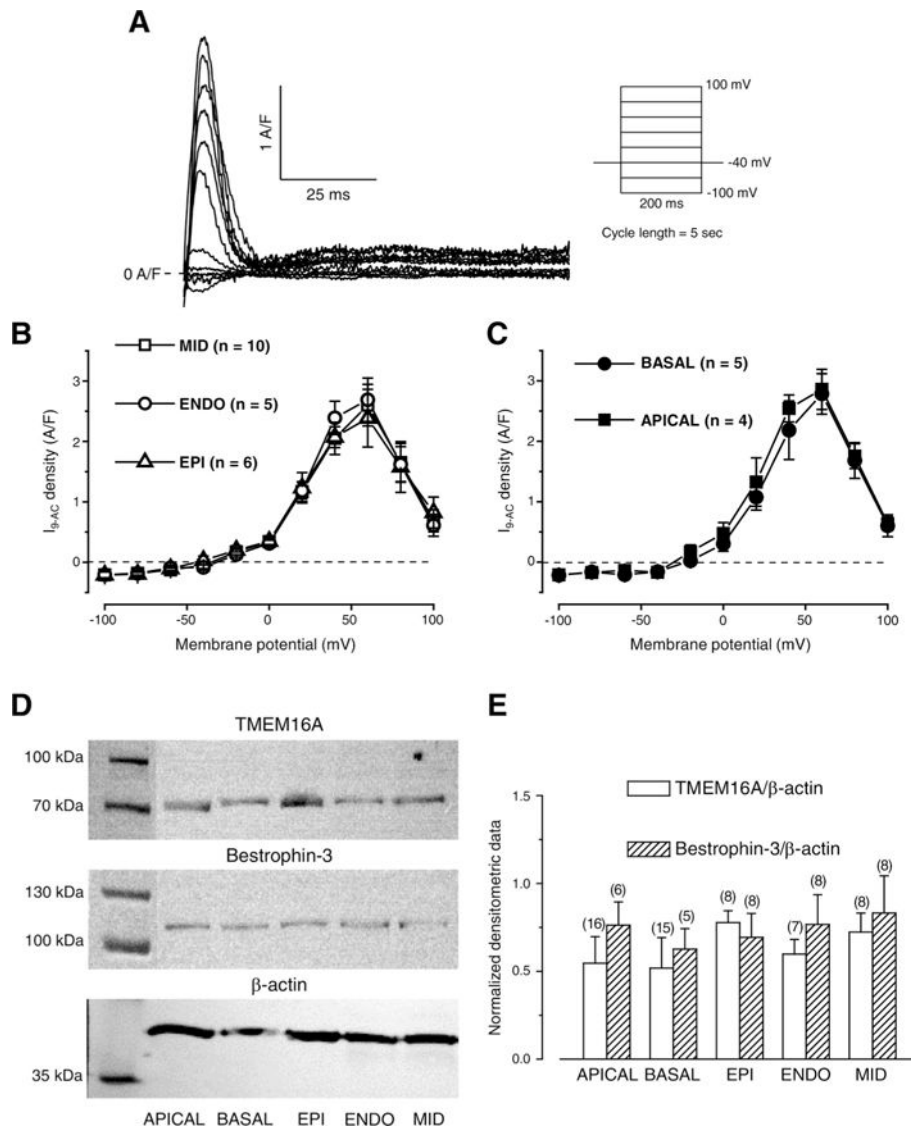
Fig. 3.
Regional I$_{Cl(Ca)}$ densities and normalized expression levels of TMEM16A and Bestrophin-3. Representative 0.5 mmol/L 9-AC-sensitive currents (I$_{9\text{-}AC}$) evoked with the stimulation protocol shown on the right side (A). Voltage dependence of I$_{9\text{-}AC}$ measured in cells obtained from various left ventricular layers (B) and from apical and basal regions of the left ventricular midmyocardium (C) using conventional square pulses. Representative Western blot images (D) showing expression of TMEM16A, Bestrophin-3, and β-actin (from top to bottom). Densitometrical values of TMEM16A (empty columns) and Bestrophin-3 (striped columns) both normalized to β-actin (E). Columns and bars indicate mean ± SEM values, n shows the number of experiments.
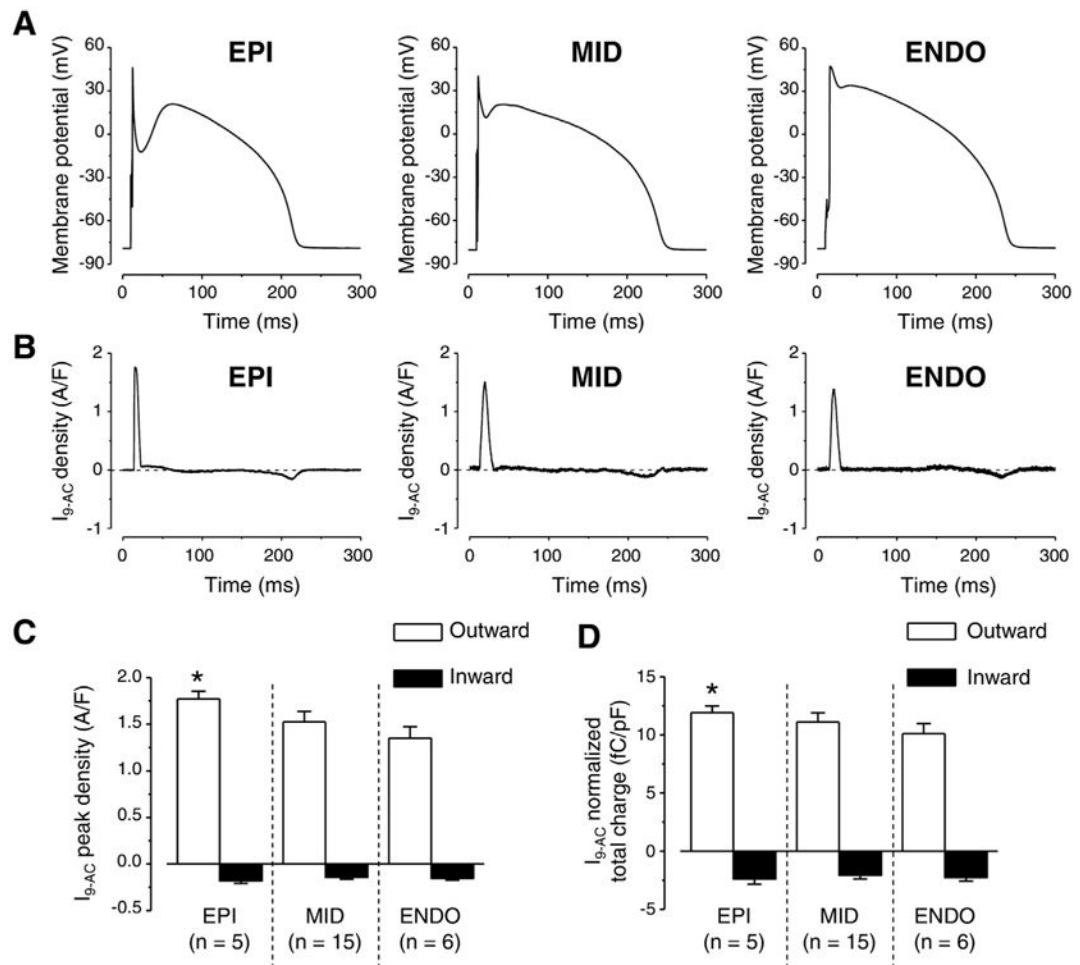
Fig. 4.

Transmural variation of $I_{Cl(Ca)}$ profiles obtained with AP voltage-clamp recordings. Representative APs obtained in EPI, MID, and ENDO cells from left to right (A) and the corresponding $I_{Cl(Ca)}$ profiles (B) recorded as 0.5 mmol/L 9-AC-sensitive currents (I_{9-AC}) are illustrated. I_{9-AC} peak densities (C) and total charges (D) measured during outward (white columns) and inward currents (black columns). Columns and bars indicate mean ± SEM values, asterisks denote significant differences between EPI and ENDO, n shows the number of experiments.
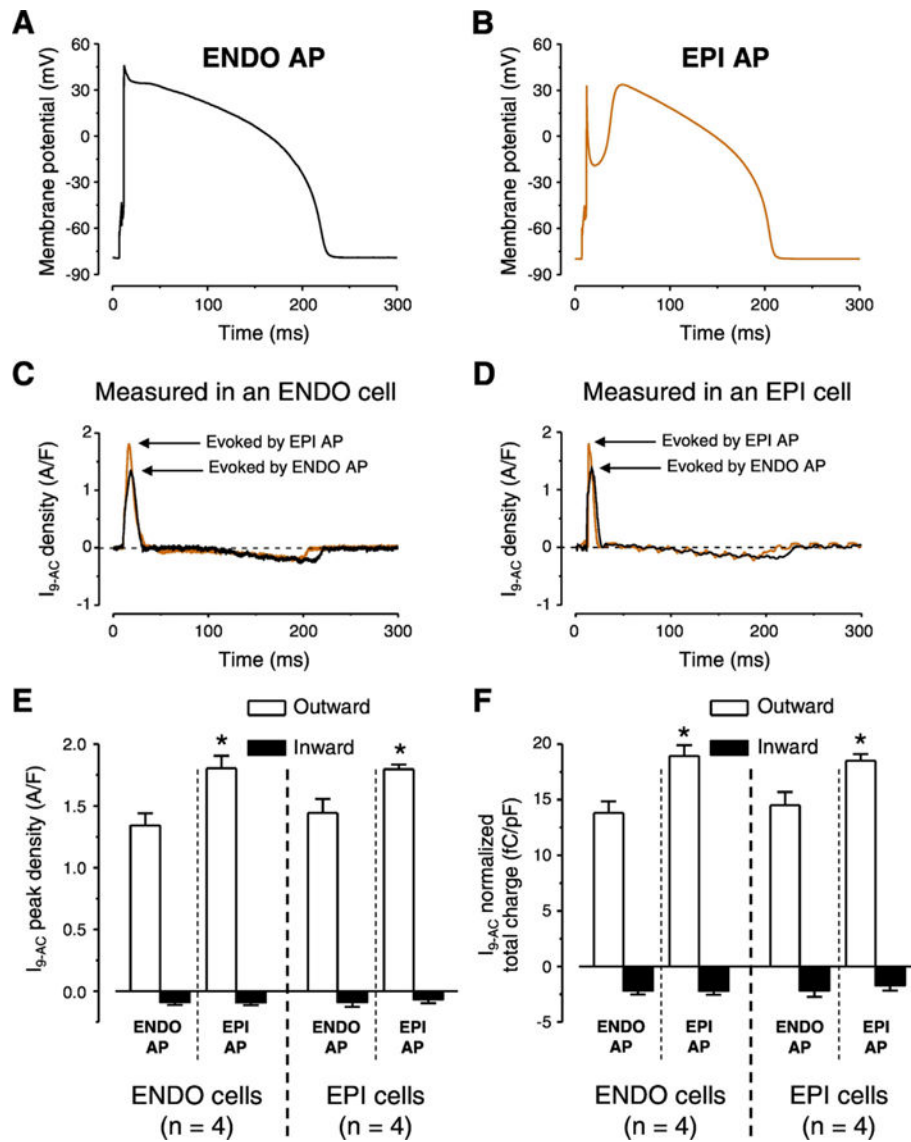
Fig. 5.

AP configuration dependent $I_{Cl(Ca)}$ profiles measured with APVC conditions. Typical ENDO (A) and EPI (B) APs used as voltage commands in cells obtained from both ENDO and EPI layers. $I_{Cl(Ca)}$ profiles recorded as 0.5 mmol/L 9-AC-sensitive currents (I_{9-AC}) in ENDO (C) and EPI cell (D) using the two typical AP waveforms. I_{9-AC} peak densities (E) and normalized total charges (F) measured during outward (white columns) and inward currents (black columns) by the indicated waveforms on given cell types. Columns and bars show mean ± SEM values. Asterisks denote significant differences between EPI and ENDO AP evoked I_{9-AC} parameters, n shows the number of experiments.
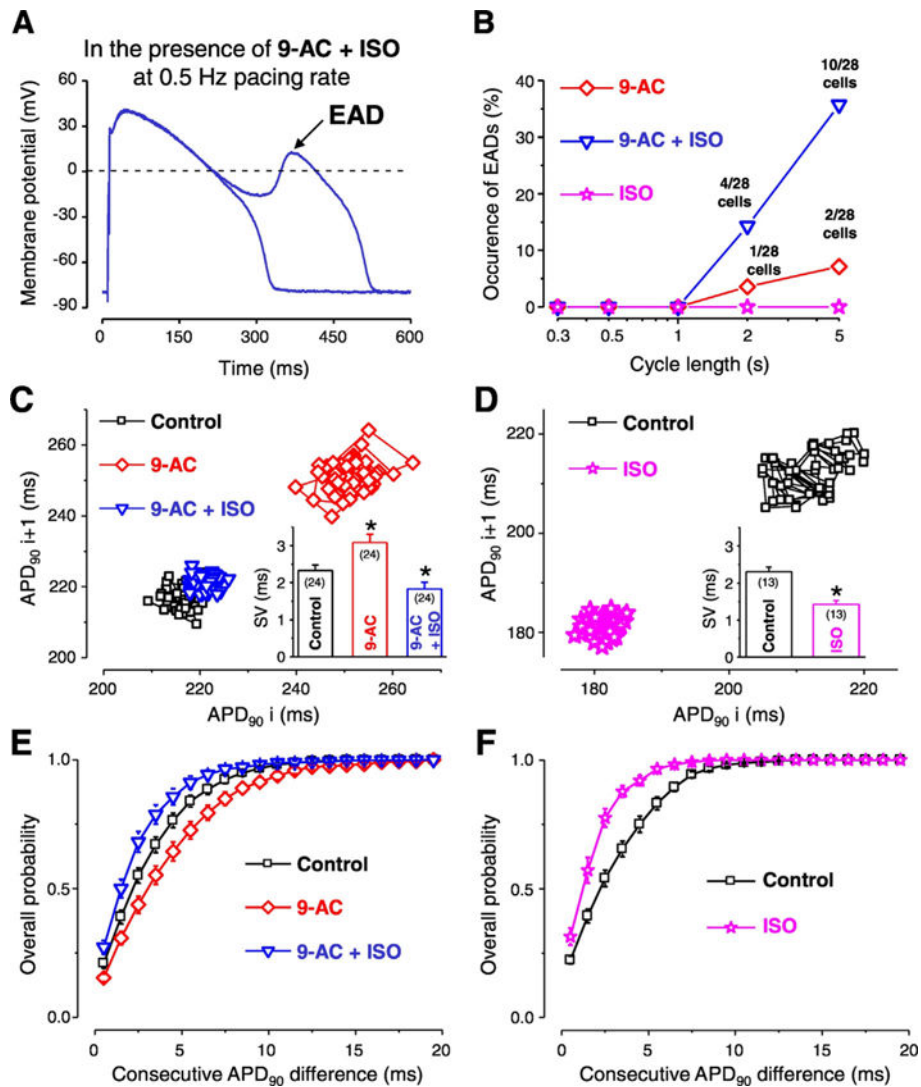
Fig. 6.
Contribution of $I_{Cl(Ca)}$ to the short-term variability of repolarization (SV) and formation of early afterdepolarization (EAD). Representative APs recorded at 0.5 Hz pacing rate in the simultaneous presence of 0.5 mmol/L 9-AC and 10 nmol/L isoproterenol (ISO) (A). Occurrence of EAD in the presence of 9-AC alone (red diamonds), ISO alone (pink stars) and in the simultaneous presence of 9-AC and ISO (blue triangles) as a function of steady-state CL (B). Representative Poincaré plots generated from 50 consecutive APs recorded in control (black squares), 9-AC (red diamonds) and in 9-AC + ISO (blue triangles) (C). On the inset of panel C the average SV values are shown. Representative Poincaré plots generated from 50 consecutive APs recorded from another cell in control (black squares) and in the presence of ISO (pink stars) and average SV values in the inset (D). Overall probability of consecutive APD_{90} differences generated from 24 measurements in control (black squares), 9-AC (red diamonds), and in 9-AC + ISO (blue triangles) conditions (E). Overall probability of consecutive APD_{90} differences generated from 13 measurements in control (black squares) and ISO (pink stars) (F). Columns, symbols and bars indicate mean ± SEM values.

Asterisks denote significant difference from control, n shows the number of experiments. (For interpretation of the references to colour in this figure legend, the reader is referred to the web version of this article.)

Table 1

AP parameters at 1 Hz stimulation rate in cells obtained from various transmural layers.

	EPI ($n = 9$)		ENDO ($n = 9$)		EPI in 4-AP ($n = 6$)		MID ($n = 20$)	
	Control	9-AC	Control	9-AC	Control	9-AC	Control	9-AC
APD_{90} (ms)	219 ± 9	208 ± 8	225 ± 10	243 ± 11	225 ± 16	241 ± 17	261 ± 9	287 ± 9
phase-1 (mV)	34.7 ± 2.6	18.1 ± 4.2	12.0 ± 2.7	1.4 ± 0.9	10.8 ± 2.7	3.5 ± 1.1	24.8 ± 1.7	9.4 ± 2.2
RMP (mV)	-80.2 ± 0.8	-80.5 ± 0.8	-79.5 ± 1.2	-81.5 ± 1.2	-79.3 ± 0.8	-80.1 ± 1.1	-80.8 ± 0.8	-81.8 ± 0.8
V_{max} (V/s)	193 ± 16	190 ± 16	184 ± 23	181 ± 21	178 ± 15	176 ± 15	190 ± 13	188 ± 12

Table 2

AP parameters at 1 Hz stimulation rate in cells obtained from apical and basal cells.

	Apical ($n = 15$)		Basal ($n = 13$)	
	Control	9-AC	Control	9-AC
APD_{90} (ms)	234 ± 9	252 ± 10	252 ± 12	282 ± 11
phase-1 (mV)	26.3 ± 2.4	16.1 ± 2.5	23.1 ± 2.0	14.0 ± 2.4
RMP (mV)	-82.6 ± 0.7	-81.6 ± 0.7	-81.3 ± 0.8	-81.4 ± 0.9
V_{max} (V/s)	205 ± 7	202 ± 8	176 ± 8	174 ± 9